Non-Cartesian MR Image Reconstruction with Integrated Gradient Nonlinearity and Off Resonance Correction

Shengzhen Tao[1], Joshua D Trzasko[1], Yunhong Shu[1], John Huston III[1], Paul T Weavers[1], and Matt A Bernstein[1]
[1]*Radiology, Mayo Clinic, Rochester, MN, United States*

Target Audience: Scientists and engineers interested in non-Cartesian image reconstruction.

Background: Conventional MRI reconstruction methods typically assume that the applied spatial encoding gradient fields vary linearly across the imaging field-of-view (FOV). In reality, however, achieving perfect gradient linearity is infeasible due to engineering limitations or concerns about peripheral nerve stimulation[1]. Gradient nonlinearity (GNL), if not explicitly accounted for, causes geometrical distortion in reconstructed images[2,3]. Conventionally, the GNL-induced geometrical distortion is corrected by image domain interpolation (e.g., "Gradwarp" on GE's system)[4]. However, direct interpolation techniques exert smoothing effects on corrected images which results in resolution loss[5-6]. In non-Cartesian MRI, B_0 inhomogeneity can also cause strong image blurring and distortion if unaccounted for during reconstruction, and is especially pronounced for long readout acquisitions[7,8]. In this work, a non-iterative gridding reconstruction framework with integrated GNL and B_0 off-resonance correction is developed for non-Cartesian MRI. As will be demonstrated, the proposed reconstruction strategy is able to mitigate the image blurring that occurs in standard interpolation-based GNL correction as well as from B_0 inhomogeneity while still effectively correcting GNL-based geometrical distortion.

Methods: In the presence of both GNL and B_0 inhomogeneity, the κ-th signal measurement for non-Cartesian MRI, $\mathbf{g}[\kappa]$, can be modeled as: $\mathbf{g}[\kappa] = \int_\Omega f(\mathbf{x}) \exp\{-j\gamma \Delta B_0(\mathbf{x}) t[\kappa]\} \exp\{-j\omega[\kappa] \Delta_{GNL}(\mathbf{x})\}\, d\mathbf{x} + \mathbf{n}[\kappa]$, where f is denotes the image object of interest, $\mathbf{x}$ is the physical position, $\Delta_{GNL}(\mathbf{x})$ is the distortion field caused by GNL which is assumed to be known *a priori*; ω denotes the non-Cartesian *k*-space trajectory; $\Delta B_0(\mathbf{x})$ denotes B_0 inhomogeneity map; $t[\kappa]$ is the readout time; and $\mathbf{n}[\kappa]$ is zero-mean proper complex Gaussian noise. Since the target quantity, f, is continuous, the problem of estimating it (under no addition assumptions) from a series of discrete signal measurement, $\mathbf{g}$, is intrinsically ill-posed. As a standard solution, a finite series approximation of f is usually employed: $f(\mathbf{x}) \approx \sum \mathbf{u}[i] b(\mathbf{x} - \mathbf{r}[i])$, where $b(\cdot)$ is the continuous pixel model, $\mathbf{u}$ is the display coefficient vector, $\mathbf{r}[i]$ is the physical position of the *i*-th pixel[9]. Assuming Dirac delta pixel model, the signal model can be expressed as $\mathbf{g}[\kappa] = \sum_{i \in \Theta} \mathbf{u}[i] \exp\{-j\gamma \Delta B_0(\mathbf{r}[i]) t[\kappa]\} \exp\{-j\omega[\kappa] \Delta_{GNL}(\mathbf{r}[i])\} + \mathbf{n}[\kappa]$, which has the affine algebraic form: $\mathbf{g} = \mathbf{A}\mathbf{u} + \mathbf{n}$. The forward operator, $\mathbf{A}$, contains the effects of off-resonance and GNL. The display coefficients vector (i.e., digital image) can be reconstructed via backprojection: $\mathbf{u} \propto \mathbf{J}_{GNL} \mathbf{A}^* \mathbf{D}_{NC} \mathbf{g}$, where $\mathbf{A}^*$ is the adjoint of $\mathbf{A}$, $\mathbf{J}_{GNL}$ is diagonal approximation of the Jacobian matrix of GNL distortion field, and $\mathbf{D}_{NC}$ is the density compensation function for non-Cartesian reconstruction. Off-resonance effects can be further decoupled from GNL effect by segmenting the *k*-space signal according to measurement time: $\mathbf{u} \propto \mathbf{J}_{GNL} \left(\sum_l \mathbf{V}_l \widehat{\mathbf{A}}^* \mathbf{W}_l\right) \mathbf{D}_{NC} \mathbf{g}$, where $\mathbf{W}_\mathbf{l}$ is a binary diagonal matrix extracting the l-th *k*-space segment based on readout time, $\mathbf{V}_l$ denotes a diagonal weighting matrix for the image reconstructed with this segment[10], and $\widehat{\mathbf{A}}^*$ represents a mapping from non-uniform *k*-space space grids to non-uniform *image* space grids for non-Cartesian MRI. The non-uniform to non-uniform mapping, $\widehat{\mathbf{A}}$, can be efficiently implemented as a type III non-uniform fast Fourier transform (NUFFT)[6,11].

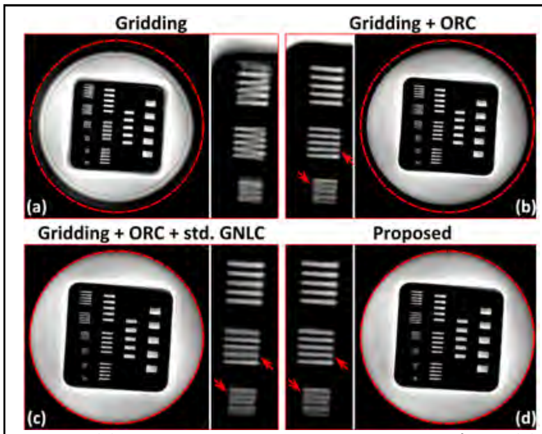

Figure 1. (a) Direct gridding reconstruction without ORC/GNLC; (b) gridding reconstruction with ORC; (c) gridding algorithm with ORC followed by standard GNLC, and (d) the proposed NUFFT based correction.

To test the proposed method, a resolution phantom was scanned at 3.0 T (GE Signa HDxt, v16.0) using zoom mode whole-body gradients (maximum gradient amplitude 40 mT/m; slew rates 200 T/m/s) and a single-channel TR head coil. The phantom was translated to -84 mm in the S/I direction, and scanned with a 2D Archimedean spiral sequence (22 cm FOV, slice thickness=3 mm, axial plane, TR=100 ms, BW=±62.5 kHz, FA=30◦, 16 interleaves, 4096 readout points per interleave). A separate 2D Cartesian dual-echo B_0 mapping sequence was then performed at the same location (22 cm FOV, Slice Thickness=3 mm, axial plane, TR = 100ms, matrix = 256 × 256, BW = ±31.25 kHz, FA = 30◦, echo spacing = 1.0ms)[7]. A B_0 map was then estimated using a graph cut based optimization procedure, and geometrically-corrected by standard methods[12]. Four separate reconstructions were performed on the same *k*-space data. Standard density-compensated gridding reconstruction with and without off resonance correction (ORC) was first performed with no GNL correction (GNLC). Standard interpolation-based GNLC was then applied to the image with ORC. Finally, the same *k*-space data was directly reconstructed with the proposed simultaneous correction method. For all cases, the reconstruction image matrix size was the same (256×256).

Results: Fig. 1 shows images (full-scale and enlargement) reconstructed by (a) density-compensated gridding without ORC/GNLC; (b) gridding with ORC; (c) gridding with ORC followed by standard GNLC, and (d) the proposed NUFFT-based simultaneous correction.

Discussion: In non-Cartesian MRI, apart from the coarse scale blurring induced by B_0 inhomogeneity, the interpolation component of standard GNL correction introduces additional image blurring, as shown in Fig. 1. By accounting for GNL and off-resonance simultaneously during reconstruction, the proposed approach is able to mitigate the blurring introduced by standard GNL correction while achieving similar correction for coarse-scale geometrical distortion and blurring induced by GNL and off-resonance. The resolution preserving effect of the proposed method is expected to be more pronounced in regions where strong GNL and off-resonance are present, e.g. at the periphery of large FOV MR acquisition[13]. The proposed reconstruction strategy also shows potential for specialized high performance gradient systems where spatial coverage and gradient linearity is sacrificed to allow higher slew rate and gradient amplitude capabilities[14]. Although only demonstrated here with a 2D spiral protocol, the proposed approach is also compatible with other 2D and 3D non-Cartesian sequences.

Conclusions: In this work, we have developed a gridding based reconstruction framework with integrated GNL and off-resonance correction for non-Cartesian MRI. The proposed method is able to mitigate the resolution loss that occurs during standard image-domain GNL correction, while still providing effective correction of coarse scale geometrical distortion and blurring induced by GNL and off-resonance.

Acknowledgment: This work was supported in part by the NIH grant 5R01EB010065.

References: [1] Harvey et al., MRM 42:561-70, 1999. [2] Schad et al., MRI 10:609-21, 1992; [3] Doran et al., Phys Med Biol 50:1343-61, 2005; [4] Glover et al., U.S. Patent 4591789, 1986; [5] Tao et al., MRM 2014, doi: 10.1002/mrm.25487; [6] Tao et al., AAPM 2014, p.SU-E-I-41; [7] King et al., MRM 34:156-60, 1995; [8] Shu et al., JMRI 30:1101-9, 2009; [9] Fessler et al., IEEE Sign Proc Mag 27: 81-9, 2010; [10] Noll et al., IEEE TMI 10:629-37, 1991; [11] Lee et al., J Comput Phys 206:1-5, 2005; [12] Kolmogorov et al., IEEE PAMI 26(2):147-159, 2004; [13] Gunter et al., Med Phys 36(6):2193-2205, 2009; [14] Mathieu et al., ISMRM 2013: 2708.